

重离子碰撞中的轻核产生和QCD相变

孙开佳^{1,2} 陈列文³ Ko Che Ming⁴ 李峰⁵ 徐骏⁶ 许长补⁷

1(复旦大学 现代物理研究所 核物理与离子束应用教育部重点实验室 上海 200433)

2(理论物理专款上海核物理理论研究中心 上海 200438)

3(上海交通大学 物理与天文学院 上海市粒子物理和宇宙学重点实验室 粒子物理与星系宇宙学教育部重点实验室 上海 200240)

4(Cyclotron Institute and Department of Physics and Astronomy, Texas A&M University, College Station, TA77843, USA)

5(兰州大学 物理科学与技术学院 兰州 730000)

6(同济大学 物理科学与工程学院 上海 200092)

7(Physics Department, Brookhaven National Laboratory, Upton, NY11973, USA)

摘要 寻找量子色动力学(Quantum Chromodynamics, QCD)相变信号是当前重离子碰撞实验的一个基础科学目标,对理解强相互作用物质的性质、大爆炸初期的宇宙演化、超新星的爆发机制、致密星的内部结构以及双中子星并合产生的引力波等重要前沿问题都具有重要意义。当重离子碰撞中发生非连续QCD相变时,引发的强相互作用物质的密度涨落与关联可以通过轻原子核的产额观察量来探测。核子间的多体关联决定了重离子碰撞中轻核的产额。特别地,基于核子并合模型对于轻核产额的计算表明质子(p)、氘核(d)和氚核(t)的产额比值 $N_t N_p / N_d^2$ 敏感于核子密度涨落与关联,是一个较好的寻找QCD相变信号的可观测量。进一步,基于输运模型对于重离子碰撞中的手征相变的模拟发现,当系统的相轨迹经过一阶相变区域时,轻核产额比值 $N_t N_p / N_d^2$ 有明显增加。这些结果为利用重离子碰撞中的轻核产生寻找QCD相变提供了理论依据。

关键词 重离子碰撞, QCD相变, 轻核产生, 并合模型, 临界涨落**中图分类号** O571.6**DOI:** 10.11889/j.0253-3219.2023.hjs.46.040012

Light nuclei production and QCD phase transition in heavy-ion collisions

SUN Kaijia^{1,2} CHEN Liewen³ Ko Che Ming⁴ LI Feng⁵ XU Jun⁶ XU Zhangbu⁷

1(Key Laboratory of Nuclear Physics and Ion-beam Application (MOE), Institute of Modern Physics, Fudan University, Shanghai 200433, China)

2(Shanghai Research Center for Theoretical Nuclear Physics, NSFC and Fudan University, Shanghai 200438, China)

3(School of Physics and Astronomy, Shanghai Key Laboratory for Particle Physics and Cosmology, Key Laboratory for Particle Physics, Astrophysics and Cosmology (MOE), Shanghai Jiao Tong University, Shanghai 200240, China)

4(Cyclotron Institute and Department of Physics and Astronomy, Texas A&M University, College Station, TA77843, USA)

5(School of Physical Science and Technology, Lanzhou University, Lanzhou 730000, China)

国家重点研发计划(No. 2022YFA1602303, No. 2022YFA1604900)、国家自然科学基金(No. 12235010, No. 11625521, No. 11922514, No. 12147101)、科技部SKA专项(No. 2020SKA0120300)资助

第一作者: 孙开佳, 男, 1988年出生, 2017年于上海交通大学获博士学位, 从事相对论重离子碰撞的物理研究

通信作者: 陈列文, E-mail: lwchen@sjtu.edu.cn

收稿日期: 2023-01-29, 修回日期: 2023-03-16

Supported by the National Key Research and Development Program of China (No. 2022YFA1602303, No. 2022YFA1604900), National Natural Science Foundation of China (No. 12235010, No. 11625521, No. 11922514, No. 12147101), the National SKA Program of China (No. 2020SKA0120300)

First author: SUN Kaijia, male, born in 1988, graduated from Shanghai Jiao Tong University with a doctoral degree in 2017, focusing on physics of relativistic heavy-ion collisions

Corresponding author: CHEN Liewen, E-mail: lwchen@sjtu.edu.cn

Received date: 2023-01-29, revised date: 2023-03-16

Abstract The searching for potential quantum chromodynamics (QCD) phase transition signals is a fundamental goal of on-going experiments on heavy-ion collisions, which is critical to understanding the properties of strongly interacting matter under extreme conditions, the inner structure of compact stars, gravitational waves emitted from neutron star mergers, etc. In particular, the beam energy scan program carried out at the Relativistic Heavy-Ion Collider (RHIC) provides a unique tool that enables studies into the QCD phase diagram and the conjectured QCD critical point. Besides the event-by-event fluctuation of conserved charges, which has been widely accepted as a useful study of the QCD critical point, the production of light nuclei can serve as a sensitive observable to the QCD phase transitions in high-energy heavy-ion collisions. The density fluctuation and correlation among nucleons are automatically encoded in the production of light nuclei in heavy-ion collisions. This study aims to demonstrate how to probe QCD phase transition with light nuclei production in heavy-ion collisions. The progress of studies in this area over the last few years is reviewed. The nucleon coalescence model provides a suitable tool for the study of the effects of density fluctuation/correlation on light nuclei production. A transport model based on the Nambu-Jona-Lasinio (NJL) model is developed to simulate the occurrence of the first-order chiral phase transition in heavy-ion collisions. Within the coalescence model for light nuclei production, the yield ratio $N_t N_p / N_d^2$ of protons (p), deuterons (d), and tritons (t) is shown to be sensitive to the nucleon density fluctuation and correlation and can function as a good probe to the non-smooth QCD phase transition. The production of light nuclei in heavy-ion collisions encodes the information about baryon density fluctuations and correlations, and enhancements of the yield ratio $N_t N_p / N_d^2$ could serve as an indicator for the occurrence of a first-order or second-order QCD phase transition.

Key words Heavy-ion collisions, QCD phase transition, Light nuclei production, Coalescence model, Critical fluctuation

描述夸克和胶子等基本粒子之间强相互作用的理论基础量子色动力学(Quantum Chromodynamics, QCD)^[1]预言,因渐进自由核物质在极端高温高密条件下会发生退禁闭相变,形成新的物质形态——夸克-胶子等离子体(Quark-Gluon Plasma, QGP)^[2-6]。强相互作用物质的热力学性质由QCD相图描述(图1(左侧))。在零重子数密度时,格点QCD的计算表明,从QGP到强子气体的转变是一种连续变化(Smooth crossover)^[7],转变温度 $T \approx 160 \text{ MeV}$ ^[8-13]。真空中自发破缺的手征对称性在高温时得到恢复。在有限重子数密度时,由于费米子符号问题,格点QCD尚无法给出确切结论。不过许多基于QCD的有效模型预言该相变将转变为一阶相变^[14-20]。QCD相图中的临界点(Critical point)正是一阶相变的终止点。除了温度和化学势,强磁场也对QCD相变的性质有着重要影响^[21-22]。利用相对论重离子碰撞寻找QGP并探索其性质是21世纪最重要的物理课题之一,对理解核物质的强相互作用、大爆炸初期的宇宙演化、超新星的爆发机制、致密星的内部结构以及双中子星并合产生的引力波等重要前沿物理问题都具有重要意义。寻找QCD相变及可能存在的临界点信号是当前高能重离子碰撞实验的一个基础科学

目标^[23-30]。

在QCD临界点附近,强相互作用物质具有较大的关联长度,可以引起守恒荷出现较强的逐事件涨落^[31-32]。近期,在位于美国布鲁克海文国家实验的相对论重离子对撞机(Relativistic Heavy Ion Collider, RHIC)上,关于净质子多重数涨落随着对撞能量依赖性的测量中发现其具有非单调性^[33],这种行为定性上与理论预期一致^[34]。尽管如此,由于重离子碰撞中的动力学十分复杂,目前仍然没有可靠的微观动力学模型计算能够定量解释净质子多重数涨落的非单调性来自于QCD临界点^[35]。因此,研究其他敏感于QCD临界点的物理量对于寻找QCD相变及临界点信号是非常重要的。

在高能重离子碰撞实验中,除了强子,人们还测量到了少量的轻原子核,如氘核(d)、氚核(t)、氦核、超核及其反核^[36-39]。这些轻核的产额与核子的密度分布以及核子间关联有紧密联系。基于核子并合模型,最近的理论研究表明,轻核产额比值 $N_t N_p / N_d^2$ 与核子密度涨落及关联之间存在十分紧密的联系,非连续QCD相变引起的重子数密度的涨落与关联可以增加 $N_t N_p / N_d^2$ 的值^[40-42]。此外,考虑到在临界点附近核子之间有效相互作用变得更加吸引,可能会出

现重子结团效应。部分结团的重子最终衰变到轻核团簇^[43]。基于这种思想,也可以证明轻核产额比值 $N_t N_p / N_d^2$ 敏感于QCD临界点附近的长程关联^[44]。因此,重离子碰撞中的轻核产生提供了一种寻找QCD相变信号的有效手段。图1给出了利用重离子碰撞

中产生的轻核寻找QCD相变信号的示意图。图中描述的是当相对论重离子碰撞产生的强相互作用物质在QCD相图中经过临界点或一阶相变区域时,能引起较大的重子数密度的涨落及关联,会随之影响末态轻核的产生。

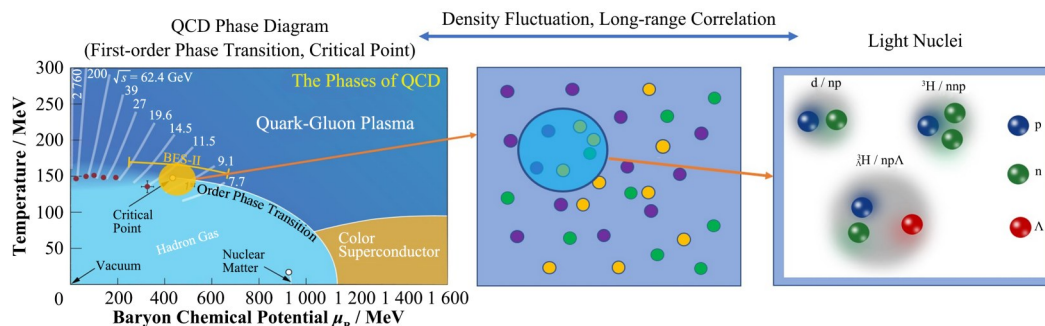


图1 利用重离子碰撞中的轻原子核产生寻找QCD相变信号的示意图
左侧相图取自文献[24]

Fig.1 Sketch of probing QCD phase transitions with light nuclei production in heavy-ion collisions
QCD phase diagram on the left is taken from Ref.[24]

相对论重离子碰撞中的QCD相变和轻核产生涉及到多个能量尺度的物理,例如 $m_N \gg \Lambda_{\text{QCD}} \sim T_c \gg E_B$,其中,核子质量 m_N 约为1 GeV, QCD能标 Λ_{QCD} 约200 MeV,夸克-强子相变温度 T_c 约为150 MeV,而轻核结合能 E_B 约为几个MeV。从空间尺度上看,满足 $R > r_{d,t} \sim (m_{d,t} E_B)^{-1/2} \sim \zeta$,其中火球半径 R 为10~20 fm,轻核半径 $r_{d,t}$ 约为2 fm,关联长度 ζ 约为几个fm^[45]。这些分析说明,轻核提供的空间分辨率可以精确到2 fm左右,与QCD临界点附近的关联长度确实是可以比的。

除了临界点信号,在重离子碰撞中寻找一阶QCD相变的信号也十分重要。如前所述,QCD相图中的一阶相变区域和临界点是密不可分的。当重离子碰撞中形成的强相互作用物质发生一阶相变时,由于力学不稳定性,会出现较大的密度非均匀性、系统膨胀放缓等效应^[46-49]。这些效应可能影响强子的HBT (Hanbury Brown and Twiss) 关联^[50]、双轻子产额^[51]、径向流^[52]以及轻核产额^[53]等可观测量。例如,研究表明,一阶QCD手征相变产生的核子密度涨落可以增加 $N_t N_p / N_d^2$ 的值^[54]。

重离子碰撞中产生的强相互作用物质处于急速膨胀之中。描述非平衡系统中的QCD相变动力学是十分必要且非常有挑战性的。针对临界涨落,人们发展了几种基于流体力学的方法,包括随机流体力学 (Stochastic Fluid Dynamics)^[55-58]、流体动力学 (Hydrokinetics)^[59-62]以及非平衡手征流体力学 (Nonequilibrium Chiral Fluid Dynamics)^[63-65]等。不

过,这些模型尚不能够定量解释实验中观测到的净质子多重数涨落的非单调性来自于QCD临界点。针对一阶相变,人们发展了基于流体力学的方法^[49]和基于输运模型的方法^[66-67]。

以下将着重介绍有关重离子碰撞中的轻核产生与QCD相变研究的近期进展。包括利用并合模型研究轻核产额比值 $N_t N_p / N_d^2$ 与核子密度涨落及关联之间的关系,一阶手征相变的动力学模拟及其对 $N_t N_p / N_d^2$ 的影响。在输运模型中,基于Nambu-Jona-Lasinio (NJL)^[68-69]模型来描述一阶手征相变^[54],并假定了退禁闭相变和手征恢复相变同时发生。通过调节夸克间的有效相互作用,可以研究具有不同临界温度的状态方程对于轻核产生的影响。这些结果为利用重离子碰撞中的轻核产生寻找QCD相变提供了理论依据。

1 核子密度涨落与关联对轻核并合产生的影响

在宇宙大爆炸核合成中,诸如氘核(d)、氚核(t)等轻原子核在温度约为1 MeV的环境中经过一系列的两体核反应过程形成^[70]。这些轻核及其反粒子也可以在重离子碰撞中形成^[36-39,71-88]。不过高能重离子碰撞中形成的强相互作用物质的温度高达100 MeV以上,远大于轻核的结合能。理解轻核形成机制有益于研究重离子碰撞中的奇特多强子态的产生^[89-90]、QGP的输运性质^[91]以及QCD相变^[40-43],也有助于间接暗物质探测^[92-97]。尽管已经有非常丰富的研究,人们依然不清楚在核-核碰撞中弱束缚

的轻核是如何形成以及它们如何在强子化后期的强子再散射中存留下来的^[98-101]。

统计强子化模型^[102-103]是一个可以很好地描述高能重离子碰撞中的粒子产生的模型。该模型假定所有的粒子,包括轻核,拥有相同的化学冻出温度和化学势。基于这样简单的假定,统计强子化模型取得了极大的成功,它可以描述在质心能量为 $\sqrt{s_{NN}} = 2.76$ TeV的Pb+Pb碰撞中从 π 介子到氦-4原子核的产额^[103]。这些粒子的产额相差达9个数量级之多。尽管如此,关于弱束缚的轻核如何在温度超过100 MeV的强子气体中存留下来依然是一个尚未解决的开放问题。

核子并合模型^[104-112]是另一个广泛应用于描述重离子碰撞中轻原子核产生的唯象模型。该模型一般假定轻核来自于强子气体演化末期核子的并合产生,这与统计强子化模型的假定形成鲜明对比。在并合模型中,轻核产额与核子的相空间分布以及核子间的关联紧密相关。此外,在并合模型中轻核的内部波函数会强烈影响其产额,而在统计强子化模型中轻核的内部结构并不重要,重要的是轻核的质量以及自旋等量子数。

尽管这两个模型取得了部分的成功,但它们都忽略了轻核产生的动力学过程。基于实时格林函数理论^[113-114],可以得到描述轻核产生的动力学过程的输运方程^[115-116],是一个描述轻核产生动力学的有效方法。

理解轻核产生机制是当前高能重离子碰撞实验特别是位于欧洲核子中心的大型强子对撞机(Large Hadron Collider, LHC)上ALICE实验的一个基本目标。随着实验数据的积累,人们已经发现了许多有关轻核产生的非常特别的现象。例如,ALICE合作组测量了从p+p、p+Pb到Pb+Pb不同碰撞系统中的轻核产生,发现在小对撞系统中轻核和超核的产额有显著的压低^[117]。这种压低可以达到一个数量级之多。ALICE合作组也首次测量了反氦核逐事件的涨落,并发现反质子和反氦核的涨落呈负相关^[118]。此外,ALICE合作组还首次测量到p+p碰撞中喷注伴随产生的氦核的并合产生概率增强了近10倍的

$$N_t = g_t \int d^3x_1 d^3x_2 d^3x_3 d^3p_1 d^3p_2 d^3p_3 f_{np}(x_1, p_1; x_2, p_2; x_3, p_3) \times W_t(x, s, p, p_s) \quad (4)$$

其中:氦核的Wigner函数为 $W_t = 8^2 \exp(-x^2 \sigma_t^{-2} - x_s^2 \sigma_t^{-2} - p^2 \sigma_t^2 - p_s^2 \sigma_t^2)$ 。坐标变换采用 $x_s = (x_1 + x_2 - 2x_3)/\sqrt{6}$, $p_s = (p_1 + p_2 - 2p_3)/\sqrt{6}$ 。宽度参数 σ_t 与氦核的均方根半径 r_t 之间的关系是 $\sigma_t = r_t = 1.59$ fm^[107-108, 120-122]。归一化条件为 $\int d^3x d^3p d^3s d^3p_s W_t(x, s, p, p_s) = (2\pi)^6$ 。三体密度联

新效应^[119]。近期,RHIC/STAR国际合作组系统测量了Au+Au碰撞中氦核和氦核产额随着能量以及中心度的依赖关系,发现氦核的产额显著低于统计强子化模型的预测^[33]。针对这些效应的理论研究,必将大大增进人们对于轻核以及其他弱束缚多强子态形成机制的认识。

1.1 轻核产生的并合模型

在以下的计算中,将采用核子并合模型计算轻核的产额,原因在于并合模型提供了研究核子密度涨落、关联与轻核产额之间关系的一个简便工具。

以氦核为例,在并合模型中其产额由中子质子联合分布函数 $f_{np}(x_1, p_1; x_2, p_2)$ 和氦核的Wigner函数 $W_d(x, p)$ 决定^[40-42, 106]:

$$N_d = g_d \int d^3x_1 d^3x_2 d^3p_1 d^3p_2 f_{np}(x_1, p_1; x_2, p_2) \times W_d(x, p) \quad (1)$$

其中: $g_d = 3/4$ 是自旋统计因子,来自于自旋1/2的质子和中子形成自旋为1的氦核。正如常在并合模型中做的一样,对氦核的Wigner函数采用高斯近似,即 $W_d = 8 \exp(-x^2 \sigma_d^{-2} - p^2 \sigma_d^2)$,其中 $x = (x_1 - x_2)/\sqrt{2}$, $p = (p_1 - p_2)/\sqrt{2}$ 。归一化条件为 $\int d^3x d^3p W_d(x, p) = (2\pi)^3$ 。宽度参数 σ_d 与氦核的均方根半径 r_d 之间的关系是 $\sigma_d = \sqrt{4/3} r_d = 2.26$ fm^[107-108, 120-122],远小于相对论重离子碰撞中产生的强子物质的尺寸。

假定具有质量为 m 的中子和质子从一个温度为 T 的热源中发射出来,对于中子质子联合分布函数可以取如下形式:

$$f_{np}(x_1, p_1; x_2, p_2) = \rho_{np}(x_1, x_2) (2\pi m T)^{-3} \exp\left(-\frac{p_1^2 + p_2^2}{2mT}\right) \quad (2)$$

其中: $\rho_{np}(x_1, x_2)$ 是坐标空间中的中子和质子联合密度分布函数,可以用单核子分布函数 ρ_n 和 ρ_p 以及两体关联函数 $C_2(x_1, x_2)$ 表达为:

$$\rho_{np}(x_1, x_2) = \rho_n(x_1) \rho_p(x_2) + C_2(x_1, x_2) \quad (3)$$

以上考虑可以推广到氦核的产生,即:

合分布函数可以进一步分解为:

$$\begin{aligned} \rho_{nnp}(x_1, x_2, x_3) = & \rho_n(x_1) \rho_n(x_2) \rho_p(x_3) + \\ & C_2(x_1, x_2) \rho_p(x_3) + C_2(x_2, x_3) \rho_n(x_1) + \\ & C_2(x_3, x_1) \rho_n(x_2) + C_3(x_1, x_2, x_3) \end{aligned} \quad (5)$$

其中忽略了两核子关联的同位旋依赖, $C_3(x_1, x_2, x_3)$ 是三核子关联函数。对于均匀分布的强子物质, C_3

仅依赖于相对坐标 $\tilde{x}_\alpha = x_1 - x_2, \tilde{x}_\beta = x_2 - x_3$, 其空间积分给出了核子数目的三阶逐事件涨落 $\langle (\delta N)^3 \rangle \propto \int d\tilde{x}_\alpha d\tilde{x}_\beta C_3$ 。因此, 当系统逐渐靠近临界点并远离时, C_3 的奇异部分将改变符号^[31]。

1.2 热力学极限

基于以上并合模型预设, 首先计算处于均匀的体积为 V 的热力学平衡系统中氘核和氚核的产额, 且假定 $C_2 = C_3 = 0$ 。由式(1)积分得到:

$$N_d \approx \frac{3}{2^{1/2}} \left(\frac{2\pi}{mT} \right)^{3/2} \frac{1}{\left(1 + \frac{1}{2mT\sigma_d^2} \right)^{3/2}} \frac{N_n N_p}{V} \quad (6)$$

$$\approx \frac{3}{2^{1/2}} \left(\frac{2\pi}{mT} \right)^{3/2} \frac{N_n N_p}{V}$$

类似地, 可以得到氚核的产额为:

$$N_t \approx \frac{3^{3/2}}{4} \left(\frac{2\pi}{mT} \right)^3 \frac{N_n^2 N_p}{V^2} \quad (7)$$

可以看出, 氘核和氚核的产额依赖于系统的温度、体积以及核子密度。进一步, 考虑如下双产额比:

$$O_{p-d-t} = \frac{N_t N_p}{N_d^2} \approx \frac{1}{2\sqrt{3}} \quad (8)$$

可以看出, 该比值是一个不依赖于系统温度和密度的常数, 这为研究其在相对论重离子碰撞中的能量依赖性提供了一个很好的基线。值得注意的是, 在重离子碰撞中产生的强相互作用物质处于急

$$N_d \approx \frac{3}{2^{1/2}} \left(\frac{2\pi}{mT} \right)^{3/2} \frac{1}{(\pi\sigma^2)^{3/2}} \int d^3 x_1 d^3 x_2 \rho_n(x_1) \rho_p(x_2) e^{-\frac{(x_1 - x_2)^2}{\sigma^2}} \quad (13)$$

$$\approx \frac{3}{2^{1/2}} \left(\frac{2\pi}{mT} \right)^{3/2} \frac{1}{(\pi\sigma^2)^{3/2}} \int d^3 X d^3 x \rho_n\left(X + \frac{x}{2}\right) \rho_p\left(X - \frac{x}{2}\right) e^{-\frac{x^2}{\sigma^2}}$$

采用梯度近似, 可以得到:

$$N_d \approx \frac{3}{2^{1/2}} \left(\frac{2\pi}{mT} \right)^{3/2} \left[\int d^3 X \rho_n(X) \rho_p(X) + \frac{1}{(\pi\sigma^2)^{3/2}} \int d^3 X d^3 x e^{-\frac{x^2}{\sigma^2}} \left[\frac{x}{2} \cdot \nabla \rho_n(X) \right] \left[\frac{x}{2} \cdot \nabla \rho_p(X) \right] \right] \quad (14)$$

当密度涨落的尺度大于轻核的尺寸时, 第二项的贡献可以忽略, 此时:

$$N_d \approx \frac{3}{2^{1/2}} \left(\frac{2\pi}{mT} \right)^{3/2} \int d^3 x \rho_n(x) \rho_p(x) \quad (15)$$

$$N_t \approx \frac{3^{3/2}}{4} \left(\frac{2\pi}{mT} \right)^3 \int d^3 x \rho_n^2(x) \rho_p(x)$$

核子密度的空间依赖可以写为:

$$\rho_n(x) = \frac{1}{V} \int \rho_n(x) d^3 x + \delta \rho_n(x) = \langle \rho_n \rangle + \delta \rho_n(x) \quad (16)$$

$$\rho_p(x) = \frac{1}{V} \int \rho_p(x) d^3 x + \delta \rho_p(x) = \langle \rho_p \rangle + \delta \rho_p(x)$$

速膨胀之中, 体积有限且密度不均匀。这些效应会使得 $N_t N_p / N_d^2$ 的值偏离 $1/(2\sqrt{3})$ 。有关 $N_t N_p / N_d^2$ 的背景贡献的详细分析见文献[123]。

统计模型或热模型可以给出一致的结果。对于化学势为 $\mu_n(\mu_p)$ 的中子(质子)密度为:

$$\rho_{np} = \frac{2}{(2\pi)^3} 4\pi T m^2 K_2 \left(\frac{m}{T} \right) e^{\frac{\mu_{np}}{T}} \quad (9)$$

其中: K_2 为二阶修正的贝塞尔函数。假定氘核和氚核与核子处于热力学平衡状态, 根据化学平衡可以得到氘核和氚核的产额分别为:

$$\rho_d = \frac{3}{(2\pi)^3} 4\pi T (2m)^2 K_2 \left(\frac{2m}{T} \right) e^{\frac{\mu_n + \mu_p}{T}} \quad (10)$$

$$\rho_t = \frac{2}{(2\pi)^3} 4\pi T (3m)^2 K_2 \left(\frac{3m}{T} \right) e^{\frac{2\mu_n + \mu_p}{T}} \quad (11)$$

很容易得到:

$$O_{p-d-t} = \frac{N_t N_p}{N_d^2} = \frac{K_2 \left(\frac{m}{T} \right) K_2 \left(\frac{3m}{T} \right)}{4 \left(K_2 \left(\frac{2m}{T} \right) \right)^2} \approx \frac{1}{2\sqrt{3}} \quad (12)$$

1.3 密度非均匀性对于轻核产生的影响

一般而言, 相对论重离子碰撞中产生的强相互作用物质的密度是不均匀的。假定核子密度 ρ_{np} 依赖于空间位置, 但不引入核子关联, 即 $C_2 = C_3 = 0$ 。此时, 氘核的并合产额近似为^[40-42]:

轻核的产额可以进一步简化为:

$$N_d \approx \frac{3}{2^{1/2}} \left(\frac{2\pi}{mT} \right)^{3/2} N_p \langle \rho_n \rangle (1 + C_{np}) \quad (17)$$

$$N_t \approx \frac{3^{3/2}}{4} \left(\frac{2\pi}{mT} \right)^3 N_p \langle \rho_n \rangle^2 (1 + 2C_{np} + \Delta \rho_n)$$

其中: C_{np} 刻画了中子、质子密度不均匀性的关联, $\Delta \rho_n$ 刻画了(坐标空间中)中子数密度的涨落^[41]。可以看出氘核和氚核的产额依赖于系统的温度、平均核子密度以及核子密度的涨落。进一步得到:

$$O_{p-d-t} \approx \frac{1}{2\sqrt{3}} (1 + \Delta \rho_n) \quad (18)$$

式(18)假定了 C_{np} 为小量。式(18)表明轻核产额比值 $N_t N_p / N_d^2$ 仅依赖于核子密度涨落, 因而是一个在重离子碰撞中寻找一阶 QCD 相变信号的理想观测量^[40-42]。

1.4 长程关联对轻核产生的影响

截至目前我们只考虑了核子密度的非均匀性对于轻核产生的影响。在QCD临界点附近,多体关联非常重要, C_2 的贡献将不可忽略。 C_2 的表达式依赖于相互作用的具体形式。对于处于临界点附近的热

力学平衡系统,临界涨落具有主导作用,对 C_2 的贡献可以不失一般性地写为^[42]:

$$C_2^{\text{critical}}(x_1, x_2) \approx \lambda \langle \rho_n \rangle \langle \rho_p \rangle \frac{e^{-|x_1 - x_2|/\xi}}{|x_1 - x_2|} \quad (19)$$

式中: ξ 是关联长度; λ 刻画了关联强度,其具体值依赖于相互作用。积分得到氘核的产额为:

$$N_d \approx \frac{3}{2^{1/2}} \left(\frac{2\pi}{mT} \right)^{3/2} N_p \langle \rho_n \rangle (1 + C_{np}) + \frac{3}{2^{1/2}} \left(\frac{2\pi}{mT} \right)^{3/2} \times \int d^3x_1 d^3x_2 C_2(x_1, x_2) \frac{e^{-\frac{(x_1 - x_2)^2}{2\sigma_d^2}}}{(2\pi\sigma_d^2)^{3/2}} \quad (20)$$

$$\approx \frac{3}{2^{1/2}} \left(\frac{2\pi}{mT} \right)^{3/2} N_p \langle \rho_n \rangle [1 + C_{np} + \frac{\lambda}{\sigma_d} G(\frac{\xi}{\sigma_d})]$$

其中:增长函数 $G(z) = \sqrt{2/\pi} - z^{-1} e^{(2z^2)^{-1}} \text{erfc}((\sqrt{2}z)^{-1})$ 随着关联长度的依赖如图2所示。

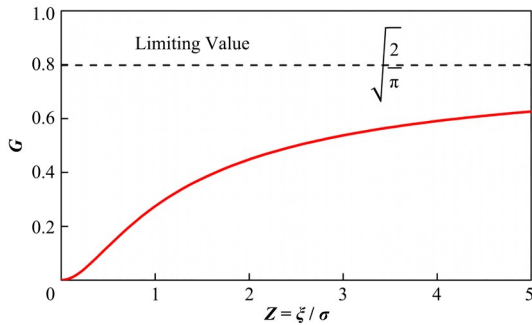


图2 增长函数 G 对于关联长度 ξ 的依赖^[42]
Fig.2 Dependence of the function $G(\xi/\sigma)$ on the correlation length ξ with σ being the width parameter in the deuteron or triton Wigner function^[42]

类似地,可以得到氚核产额的表达式:

$$N_t \approx \frac{3^{3/2}}{4} \left(\frac{2\pi}{mT} \right)^3 N_p \langle \rho_n \rangle^2 [1 + \Delta\rho_n + 2C_{np} + \frac{3\lambda}{\sigma_t} G(\frac{\xi}{\sigma_t}) + O(G^2)] \quad (21)$$

以及轻核产额比值:

$$O_{p-d-t} \approx \frac{1}{2\sqrt{3}} [1 + \Delta\rho_n + \frac{\lambda}{\sigma} G(\frac{\xi}{\sigma})] \quad (22)$$

其中: $\sigma \approx \sigma_d \approx \sigma_t$ 。可以看出,随着关联长度的增加,该比值单调增加。式(22)表明 $N_t N_p / N_d^2$ 可以用于在重离子碰撞中寻找QCD临界涨落的信号^[42]。

2 基于输运模型研究QCD一阶相变对于轻核产生的影响

在上述计算中,假定了QCD相变产生的密度非均匀性和长程关联可以在强子气体的膨胀演化中存留至末态。为了更加定量地研究QCD相变对于轻核产生的影响,构建能够描述QCD相变动力学的微观模型是非常重要的。由于非微扰效应,求解有限

密度有限温度的QCD动力学是十分困难的。人们广泛采用QCD的低能有效理论NJL^[68-69]模型来描写手征对称性的破缺与恢复。以下采用基于NJL模型的微观输运模型来描述相对论重离子碰撞的动力学演化,并研究一阶手征相变对于轻核产生的影响。

2.1 NJL 模型

采用三味NJL模型描述部分子间的相互作用,其拉格朗日密度为^[124]:

$$\mathcal{L} = \mathcal{L}_0 + \mathcal{L}_S + \mathcal{L}_V + \mathcal{L}_{\text{det}} \quad (23)$$

其中:

$$\mathcal{L}_0 = \bar{\psi} (i\gamma^\mu \partial_\mu - \hat{m}) \psi$$

$$\mathcal{L}_S = G_S \sum_{a=0}^8 [(\bar{\psi} \lambda^a \psi)^2 + (\bar{\psi} i\gamma^5 \lambda^a \psi)^2] \quad (24)$$

$$\mathcal{L}_V = -g_V (\bar{\psi} \gamma^\mu \psi)^2$$

$$\mathcal{L}_{\text{det}} = -K [\det \bar{\psi} (1 + \gamma_5) \psi + \det \bar{\psi} (1 - \gamma_5) \psi]$$

式中: \mathcal{L}_0 是自由夸克的拉格朗日密度; $\psi = (u, d, s)^T$ 是夸克场; $\hat{m} = \text{diag}(m_u, m_d, m_s)$ 是流夸克质量矩阵; \mathcal{L}_S 是标量相互作用的拉格朗日密度; G_S 是标量耦合常数; $\lambda^a (a=1, \dots, 8)$ 是Gell-Mann矩阵, $\lambda^0 = \sqrt{2/3} I$; \mathcal{L}_{det} 是Kobayashi-Maskawa-t' Hooft (KMT)相互作用^[125],其破缺了 $U(1)_A$ 对称性。在味空间求行列式:

$$\det (\bar{\psi} \Gamma \psi) = \sum_{i,j,k} \varepsilon_{ijk} (\bar{u} \Gamma q_i) (\bar{d} \Gamma q_j) (\bar{s} \Gamma q_k) \quad (25)$$

给出了味空间六顶点相互作用。 \mathcal{L}_V 代表夸克间的矢量相互作用, g_V 是耦合常数^[126]。

利用平均场近似^[127],拉格朗日密度可以写成:

$$\mathcal{L} = \bar{u} (\gamma^\mu iD_\mu - M_u) u + \bar{d} (\gamma^\mu iD_\mu - M_d) d + \bar{s} (\gamma^\mu iD_\mu - M_s) s - 2G_S (\phi_u^2 + \phi_d^2 + \phi_s^2) + 4K \phi_u \phi_d \phi_s + g_V (j_u^\mu + j_d^\mu + j_s^\mu) (j_{\mu u} + j_{\mu d} + j_{\mu s}) \quad (26)$$

其中:

$$M_u = m_u - 4G_S \phi_u + 2K \phi_d \phi_s$$

$$M_d = m_d - 4G_S \phi_d + 2K \phi_u \phi_s$$

$$M_s = m_s - 4G_S \phi_s + 2K \phi_u \phi_d \quad (27)$$

式(27)是介质中的夸克质量。 $\phi_u = \langle \bar{u}u \rangle$ 、 $\phi_d = \langle \bar{d}d \rangle$ 和 $\phi_s = \langle \bar{s}s \rangle$ 是夸克的凝聚。 $j_{u\mu} = \langle \bar{u}\gamma_\mu u \rangle$ 、 $j_{d\mu} = \langle \bar{d}\gamma_\mu d \rangle$ 和 $j_{s\mu} = \langle \bar{s}\gamma_\mu s \rangle$ 是净夸克矢量流。协变导数为 $iD_\mu = i\partial_\mu - A_\mu$,其中:

$$A_\mu = 2g_V(j_{u\mu} + j_{d\mu} + j_{s\mu}) \quad (28)$$

2.2 状态方程

三味夸克系统的热力学性质可以通过配分函数 Z 得到, Z 的路径积分表示是:

$$Z = \text{Tr} e^{-\frac{1}{T}(\hat{H} - \mu\hat{N})} = \int D\psi D\bar{\psi} e^{\int_0^\beta \int d^3x \mathcal{L}} \quad (29)$$

其中: $\beta = 1/T$ 和 \hat{H} 分别是温度的倒数和哈密顿量算符; μ 和 \hat{N} 分别是化学势和相应的守恒荷的粒子数算符。体积为 V 的夸克物质的热力学势是:

$$\Omega = -\frac{T}{V} \ln Z = \Omega_u + \Omega_d + \Omega_s + 2G_S(\phi_u^2 + \phi_d^2 + \phi_s^2) - 4K\phi_u\phi_d\phi_s - g_V(\rho_u + \rho_d + \rho_s)^2 \quad (30)$$

其中: $\rho_{i=u,d,s}$ 是夸克的净粒子数密度。

$$\varepsilon = -\frac{\partial \Omega}{\partial T} \Omega + \beta \frac{\partial \Omega}{\partial \beta} + \sum_{i=u,d,s} \mu_i \rho_i - \varepsilon_0$$

$$= -2N_c \sum_{i=u,d,s} \int_0^\Lambda \frac{d^3p}{(2\pi)^3} E_i (1 - n_i - \bar{n}_i) + 2G_S(\phi_u^2 + \phi_d^2 + \phi_s^2) - 4K\phi_u\phi_d\phi_s + g_V(\rho_u + \rho_d + \rho_s)^2 - \varepsilon_0 \quad (34)$$

其中:引入 ε_0 是为了保证真空中 $\varepsilon = 0$ 。熵密度和自由能密度分别是 $s = (\varepsilon + P - \sum_{i=u,d,s} \mu_i \rho_i)/T$ 和 $f = \varepsilon - Ts$ 。NJL模型中使用的参数如下:

$m_u = m_d = 5.5 \text{ MeV}$, $m_s = 140.7 \text{ MeV}$, $G_S A^2 = 1.835$, $KA^5 = 12.36$ 和 $A = 602.3 \text{ MeV}$ ^[124, 128-129]。

图3展示了无矢量相互作用时温度-密度平面中夸克物质的相图。点划线代表了手征恢复与破缺相共存线,而实线包围的区域是力学不稳定区间($(\partial P/\partial \rho_q)_T < 0$)。临界点对应的温度和净夸克数密度大约分别是67 MeV和0.85 fm⁻³。当矢量相互作用常数取 $g_V = G_S$,相图中的临界点消失,从手征恢复相到破缺相的转变完全是连续变化(Crossover)。在相对论重离子碰撞的真实体系中,由于 u 和 d 夸克的化学势差别很小,化学不稳定性不重要^[130],上述讨论仍然成立。

2.3 输运方程

我们还需要了解处于非平衡状态下,特别是相变过程中,强相互作用物质的性质。基于以上NJL模型,可以写出夸克相空间分布函数随时间的演化方程^[131-132]:

$$\Omega_i = -2N_c \int \frac{d^3p}{(2\pi)^3} [E_i + T \ln(1 + e^{\frac{E_i - \mu_i^*}{T}}) + T \ln(1 + e^{\frac{E_i + \mu_i^*}{T}})] \quad (31)$$

其中: $E_i = (M_i^2 + p^2)^{1/2}$ 和 $\mu_i^* = \mu_i - 2g_V(\rho_u + \rho_d + \rho_s)$ 分别是夸克能量和有效化学势。

通过有效质量和化学势对于热力学势做最小化($\delta \Omega/\delta M_i = \delta \Omega/\delta \mu_i^* = 0$)可以得到夸克凝聚和净夸克数密度,即:

$$\phi_i = 2N_c \int \frac{d^3p}{(2\pi)^3} \frac{M_i}{E_i} (n_i + \bar{n}_i - 1) \quad (32)$$

$$\rho_i = 2N_c \int \frac{d^3p}{(2\pi)^3} \frac{p_\mu}{E_i} (n_i - \bar{n}_i)$$

其中:夸克和反夸克的分布函数为 $n_i = (e^{\frac{E_i - \mu_i^*}{T}} + 1)^{-1}$ 和 $\bar{n}_i = (e^{\frac{E_i + \mu_i^*}{T}} + 1)^{-1}$ 。净夸克数密度 ρ_i 是净夸克流四矢量的时间分量:

$$j_{i\mu} = 2N_c \int \frac{d^3p}{(2\pi)^3} \frac{p_\mu}{E_i} (n_i - \bar{n}_i) \quad (33)$$

由于NJL模型是不可重整化的,通常在积分中引入动量截断 Λ 。能量密度为:

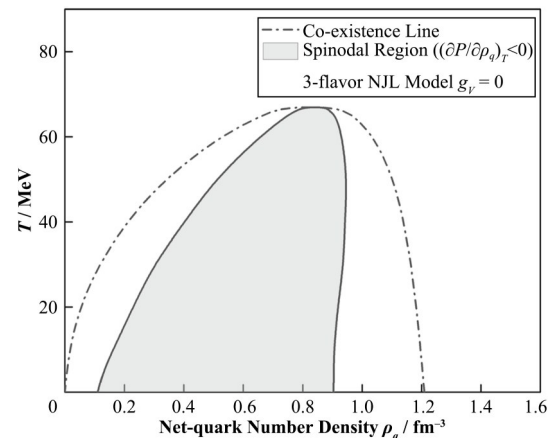


图3 NJL模型中夸克物质相图(温度-密度平面)^[54]
Fig.3 Quark matter phase diagram in the temperature and the net-quark density plane from the three-flavor NJL model ($g_V = 0$) with equal chemical potential for u and d quarks and zero chemical potential for s quarks^[54]

$$\frac{\partial f_\pm}{\partial t} + v \cdot \nabla_r f_\pm + \left(-\frac{M}{E^*} \nabla_r M \pm E \pm v \times B \right) \cdot \nabla_p f_\pm = \left(\frac{\partial f_\pm}{\partial t} \right)_{\text{coll}} \quad (35)$$

其中:强相互作用电磁场为 $E = -\partial A/\partial t + \nabla_r A_0$ 和 $B = \nabla_r \times A$ 。其中 A_μ 的定义见式(28)。介质中分子的能量是 E^* ,速度是 $v = p/E^*$ 。碰撞积分为:

$$\left(\frac{\partial f_{\pm}}{\partial t}\right)_{\text{coll}} = -\frac{1}{(2\pi)^3} \iint dp_2 dp_3 \int d\Omega |v_{12}| \frac{d\sigma}{d\Omega} \delta^{(3)}(p + p_2 - p_3 - p_4) \times \{ f_{\pm}(r, p, t) f(r, p_2, t) \times [2N_c - f(r, p_3, t)] [2N_c - f(r, p_4, t)] - f(r, p_3, t) f(r, p_4, t) [2N_c - f_{\pm}(r, p, t)] [2N_c - f(r, p_2, t)] \} \quad (36)$$

式中： $f(r, p, t)$ 是夸克或者反夸克的相空间分布函数； v_{12} 是两个散射夸克的相对速度； $d\sigma/d\Omega$ 是微分散射截面。

输运方程可以用试验粒子方法^[133]求解，每个试验部分子的运动包括在平均场中的受力运动和部分子之间的散射。试验部分子的运动方程是：

$$\begin{aligned} \frac{dr}{dt} &= v \\ \frac{dp}{dt} &= -\frac{M}{E^*} \nabla_r M \pm E \pm v \times B \end{aligned} \quad (37)$$

在试验粒子方法中，对于动量超过动量截断 Λ 的部分子不计入部分子的标量和矢量密度的计算中，也不参与平均场相互作用。在以下计算中，试验粒子数目是100，计算标量和矢量密度的格点大小空间是1 fm×1 fm×1 fm。为了压低平均场的统计涨落，标量和矢量密度取临近3×3×3格点的平均值。利用试验粒子的方法求解输运方程时，时间步长取 $\Delta t = 0.2 \text{ fm} \cdot \text{c}^{-1}$ 。

2.4 盒子计算

我们先考虑无穷大核物质中一阶相变的动力学演化，然后计算有限系统重离子碰撞中的情形。我们选取具有周期性边界条件大小为20 fm×20 fm×20 fm的格子来模拟无穷大夸克物质。夸克物质的初始净夸克数密度和温度分别为0.7 fm⁻³和40 MeV。如图4所示，当 $t = 0 \text{ fm} \cdot \text{c}^{-1}$ 时夸克均匀地分布在盒子中，仅有的涨落来自统计效应。随着时间的演化，由于夸克物质处于相图中的力学不稳定区间，初始的统计涨落被逐渐放大，进而发生结团形成较大的密度涨落。当 $t = 100 \text{ fm} \cdot \text{c}^{-1}$ 时结团效应已经非常明显。图5进一步给出了密度二阶矩 $y_2 = [\int dx (\rho(x))^3] / [\int dx \rho(x)] / [\int dx (\rho(x))^2]^2$ ^[54]和温度差随着时间的演化。 y_2 的值先缓慢增加，然后快速增加到约1.15。随着结团效应的出现，系统潜热得到释放，温度增加。不过温度只增加了最多3 MeV，该效应在重离子碰撞中可能较难观测到。

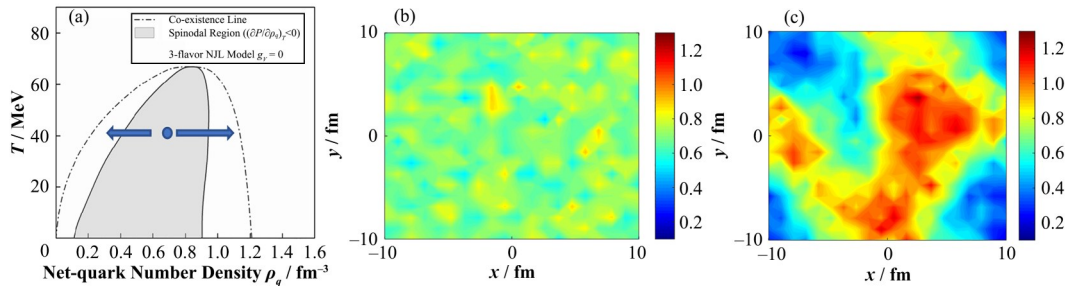


图4 NJL模型中夸克物质相图(a)， $t=0 \text{ fm} \cdot \text{c}^{-1}$ 时夸克物质密度分布(b)， $t=100 \text{ fm} \cdot \text{c}^{-1}$ 时夸克物质密度分布(c)^[54]
Fig.4 Quark matter phase diagram in the temperature and net-quark density plane from the three-flavor NJL model (a), quark matter density at $t = 0 \text{ fm} \cdot \text{c}^{-1}$ (b) and $100 \text{ fm} \cdot \text{c}^{-1}$ (c)^[54]

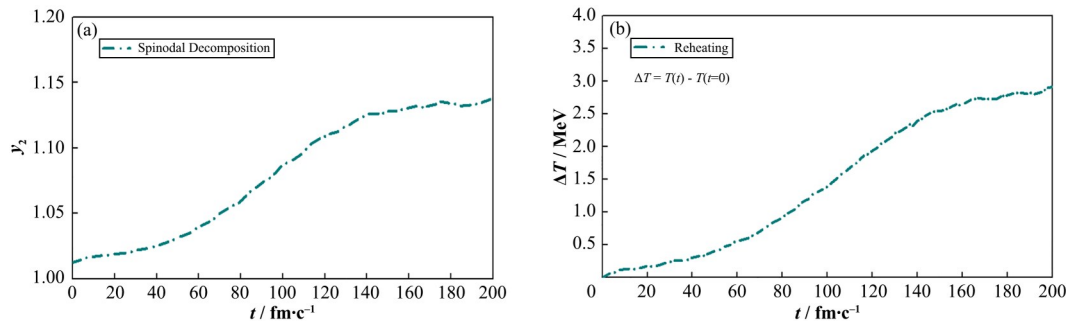


图5 夸克物质密度二阶矩和温度差随着时间的依赖
Fig.5 Time dependence of the second-order scaled density moment and temperature difference

2.5 重离子碰撞模拟

现在考虑重离子碰撞中一阶QCD相变对于轻核产生的影响，假定初始的夸克、反夸克服从

Woods-Saxon分布：

$$\rho(r) = \frac{\rho_0}{1 + \exp((r - R)/a)} \quad (38)$$

其中： $R = 6 \text{ fm}$ ，表面厚度参数是 $a = 0.6 \text{ fm}$ ，中心夸

克净夸克密度是 $\rho_0 = 1.5 \text{ fm}^{-3}$ 。初始温度是 70 MeV, 化学势满足 $\mu_u = \mu_d$ 及 $\mu_s = 0$ 。我们考虑两种相互作用情形 $g_V = 0$ 和 $g_V = G_S$ 。

对于矢量相互作用为 0 的情形 ($g_V = 0$), 其对应的状态方程的临界温度约为 67 MeV。图 6 展示了净夸克数密度分布及其二阶矩 y_2 随时间的演化。可以看出在部分子阶段, 随着系统的膨胀 y_2 急剧增加, 这意味着系统发展出了较大的密度不均匀性。而对于 $g_V = G_S$ 的情形, 如图 7 所示, 随着系统的膨胀 y_2 维持在一个常数 1.25 附近, 系统的密度不均匀性没

有发生显著的改变。

图 8 给出了重子数密度分布的二阶矩 y_2 对时间的依赖。实线和虚线分别对应了 $g_V = 0$ 和 $g_V = G_S$ 两种情形。强子化发生在五角星对应的时刻。可以看出当一阶相变发生时, y_2 的值超过了 2, 在强子演化阶段也仅微弱下降, 说明密度涨落在火球膨胀的过程中存留了下来。这类似于宇宙大爆炸早期量子涨落引起的温度不均匀性在宇宙的快速膨胀中存留了下来。今天可以清楚地观测到宇宙微波背景的非均匀性。而当发生连续相变时, 密度的不均匀性在火球的整个演化中没有明显的变化。

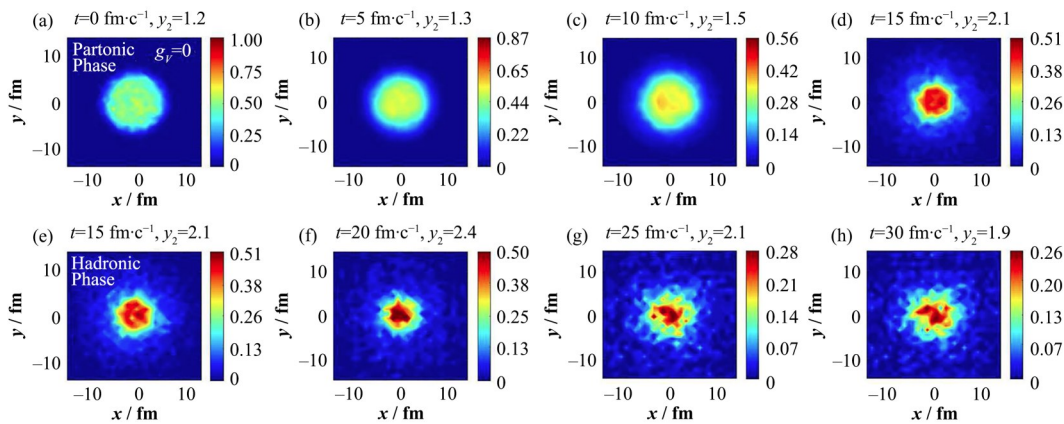


图 6 净夸克数密度分布及其二阶矩随时间的演化 ($g_V = 0$)^[54] (a~d) 部分子阶段, (e~h) 强子相阶段
Fig.6 Evolution of the distribution of net-baryon number density in fm^{-3} and the second-order scaled density moment y_2 in the transverse plane $z = 0$ in the partonic phase (a~d) and the hadronic phase (e~h) for the case of $g_V = 0$ ^[54]

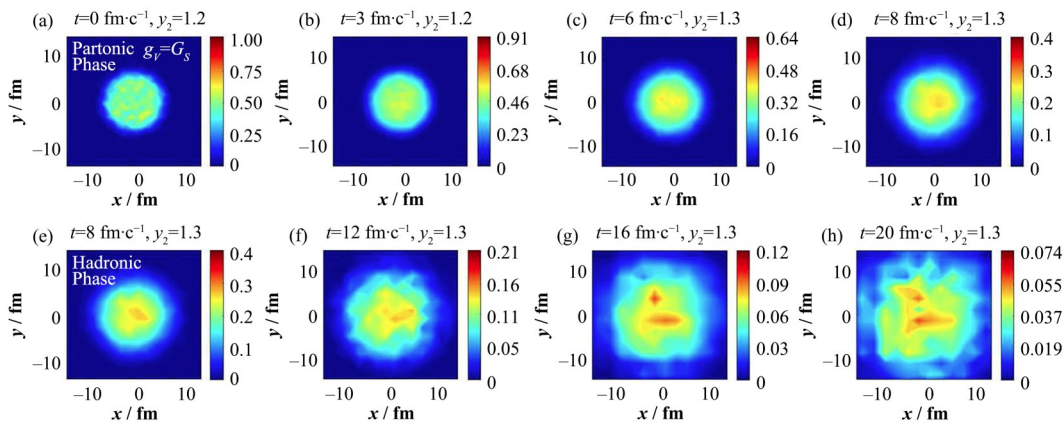


图 7 净夸克数密度分布及其二阶矩随时间的演化 ($g_V = G_S$)^[54] (a~d) 部分子阶段, (e~h) 强子相阶段
Fig.7 Evolution of the distribution of net-baryon number density in fm^{-3} and the second-order scaled density moment y_2 in the transverse plane $z = 0$ in the partonic phase (a~d) and the hadronic phase (e~h) for the case of $g_V = G_S$ ^[54]

图 9 进一步给出了相图中部分子相的演化径迹。径迹上的点代表系统的平均温度和平均净夸克密度。每个格点的温度根据状态方程以及格点上的能量密度和重子数密度求解得到。计算相径迹时取每个格点中的夸克数目作为权重。对于 $g_V=0$ 的情形, 可以看出在 $t=4 \text{ fm} \cdot \text{c}^{-1}$ 时, 系统演化至 Spinodal

不稳定区域, 此时约有 65% 的夸克的质量小于 200 MeV, 夸克的平均质量约为 165 MeV。随着系统的膨胀, 密度涨落逐渐增加, 在 $t=15 \text{ fm} \cdot \text{c}^{-1}$ 时 $y_2 = 2$, 夸克平均质量增加至约 270 MeV, 这相当于夸克真空质量的 70%。此时, 大约有 70% 的夸克质量超过 200 MeV, 系统温度约为 30 MeV。对于 $g_V = G_S$

的情形,系统大约经过 $8 \text{ fm} \cdot \text{c}^{-1}$, 约 70% 的夸克质量会超过 200 MeV。

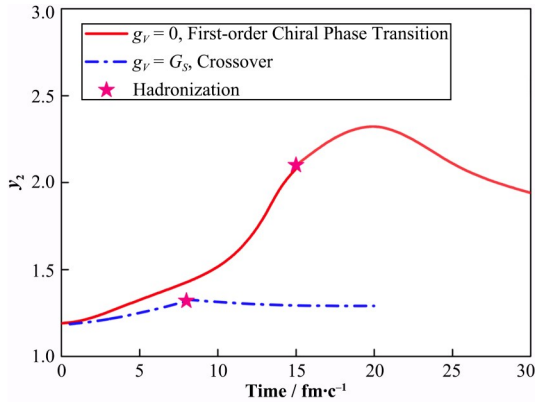


图8 密度分布的二阶矩 y_2 对时间的依赖^[54]

Fig.8 Time dependence of the second-order scaled moment y_2 of net-baryon density for the two cases of $g_V=0$, with a first-order chiral phase transition (solid line) and $g_V=G_S$ with a smooth crossover (dash-dotted line)^[54]

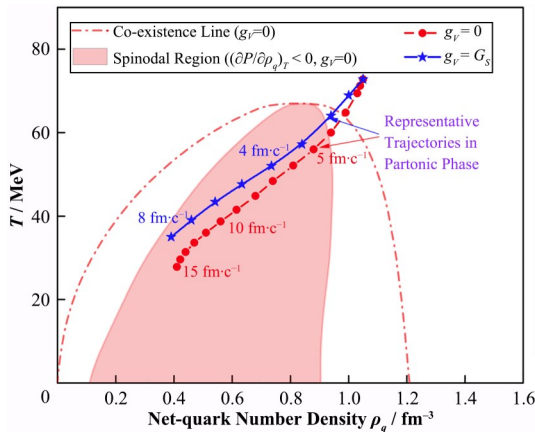


图9 相空间径迹演化^[54]

Fig.9 Evolution of phase trajectory in the phase diagram for $g_V=0$ with a first-order chiral phase transition (solid circles) and $g_V=G_S$ with a smooth crossover (solid stars)^[54]

基于演化末态的核子相空间分布函数,利用核子并合模型计算得到轻核产额。图 10 给出了轻核产额比值 $N_t N_p / N_d^2$ 随着状态方程的依赖。当 $g_V=0$ 时,系统的相空间径迹在火球膨胀的过程中经过一阶相变区域,演化出了较大的密度非均匀性。此时 $N_t N_p / N_d^2$ 的值达到了 0.50 左右。而当 $g_V=G_S$ 和 $g_V=2G_S$ 时,相图中只有连续变化,没有一阶或者二阶相变。此时 $N_t N_p / N_d^2$ 的值约为 0.38。可以看出,由于发生了一阶相变, $N_t N_p / N_d^2$ 的值增加了约 25%。与之前解析推导不同,在图 10 中核子并合计算的结果里没有采用任何近似。

2.6 $N_t N_p / N_d^2$ 能量依赖的初步结果

以上的模型计算表明,重离子碰撞中的一阶

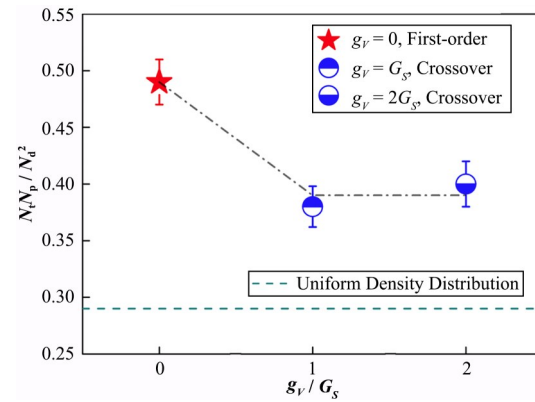


图 10 轻核产额比值 $N_t N_p / N_d^2$ 对状态方程的依赖^[54]

Fig.10 Yield ratio $N_t N_p / N_d^2$ of proton (p), deuteron (d), and triton (t) for the cases of $g_V=0$ with a first-order phase transition (solid star) as well as $g_V=G_S$ and $g_V=2G_S$ with a crossover transition (circles)^[54]

QCD 相变可以导致轻核产额比值 $N_t N_p / N_d^2$ 出现显著增加。不同的对撞能量可以扫描相图中的不同区域,因而可以利用重离子碰撞能量扫描实验来寻找一阶 QCD 相变的信号。不过,由于以上 NJL 模型中临界点的温度最大仅有 70 MeV 左右,不适合用于能量扫描实验。

近期,通过引入标量-矢量耦合相互作用^[134],我们成功发展了基于拓展 NJL 模型的部分子输运模型^[135]。该拓展 NJL 模型的临界温度可以高达 150 MeV 左右,适合应用于 RHIC 能量扫描实验。计算表明,在 $\sqrt{s_{NN}} > 5 \text{ GeV}$ 时,不同的状态方程给出的 $N_t N_p / N_d^2$ 相差无几。当 $\sqrt{s_{NN}} < 5 \text{ GeV}$ 时,状态方程对应的临界温度越高, $N_t N_p / N_d^2$ 的值越大。当临界温度大于 140 MeV 时, $N_t N_p / N_d^2$ 的值与实验测量比较一致。

对于一些没有临界效应和一阶相变效应的模型计算例如 JAM+COAL^[140]、AMPT+COAL^[136]、UrQMD+COAL^[137]、MUSIC+UrQMD+COAL^[138] 等, $N_t N_p / N_d^2$ 的值随着对撞能量的依赖几乎是平的。在 $\sqrt{s_{NN}} > 20 \text{ GeV}$ 时,STAR 合作组最新实验数据^[139]中有疑似非单调行为存在,不过目前尚无模型计算能够定量描述这一现象。一种可能性是由于临界点附近的长程关联导致 $N_t N_p / N_d^2$ 在特定的对撞能量的重离子碰撞中增强(见式(22))^[42]。

3 结果和讨论

基于核子并合模型的计算发现轻核产额依赖于末态核子的密度涨落与关联。特别地,核子的密度涨落与长程关联可以增加轻核产额比 $N_t N_p / N_d^2$ 的值。

为了探索一阶QCD相变引起的密度非均匀性在重离子碰撞中的动力学演化,我们发展了基于NJL模型的相对论输运模型。计算发现,由于系统的快速膨胀,一阶相变产生的密度涨落可以存留至系统演化的末期,导致并合产生的轻核产额比 $N_t N_p / N_d^2$ 的值增加约25%。这些结果为在重离子碰撞中寻找QCD相变信号提供了理论依据和定量参考。

最近,我们进一步发展了基于扩展NJL模型的输运模型。在该模型中,通过调节标量-矢量相互作用的耦合强度可以改变临界点的位置,临界温度可以从40 MeV调节到150 MeV左右。通过对碰撞能量、碰撞中心度以及临界点位置的扫描,我们发现在对撞能量为 $\sqrt{s_{NN}} \approx 3\sim 5$ GeV的Au+Au碰撞中一阶QCD相变会大大增加 $N_t N_p / N_d^2$ 的值。这与STAR国际合作组的初步测量是一致的。

由于采用了平均场近似以及试验粒子方法,目前的输运模型只能描述单粒子分布函数随时间的演化,无法精确描述两粒子关联函数的演化,因而我们仅研究了一阶相变的效应。如何利用输运模型刻画临界涨落是一个很有挑战性的问题。此外,目前基于NJL相互作用的输运模型中只有夸克自由度,没有胶子自由度。如何引入胶子自由度,并自洽计算其动力学演化也是一个重要且很有挑战性的课题^[141]。

当重离子碰撞中发生非连续的QCD相变,系统的动力学随之发生改变,将会对许多物理量产生影响。我们仔细讨论了QCD相变对于重离子碰撞中轻核产额的影响。除了轻核,还可以研究QCD相变对于集体流^[52]、HBT关联^[50]、双轻子产生^[51]、 ρ 介子产生^[142],以及自旋排列^[143]等物理量的影响。这些方面的工作正在进展中。

4 结语

模型计算表明重离子碰撞中发生的非连续的QCD相变会影响轻核的产生,特别是可以增加轻核产额比 $N_t N_p / N_d^2$ 的值。利用该效应在重离子碰撞中寻找可能的QCD相变信号是一个非常值得探索的方向。未来。在此方向上还有许多重要的理论工作值得开展,例如厘清重离子碰撞中轻核产生机制和QCD相变的动力学效应等。

作者贡献声明 本文作者对文章的完成均作出了同等重要的贡献。

参考文献

- 1 Fritzsche H, Gell-Mann M, Leutwyler H. Advantages of the color octet gluon picture[J]. *Physics Letters B*, 1973, **47**(4): 365 – 368. DOI: 10.1016/0370-2693(73)90625-4.
- 2 Collins J C, Perry M J. Superdense matter: neutrons or asymptotically free quarks? [J]. *Physical Review Letters*, 1975, **34**(21): 1353 – 1356. DOI: 10.1103/physrevlett.34.1353.
- 3 Cabibbo N, Parisi G. Exponential hadronic spectrum and quark liberation[J]. *Physics Letters B*, 1975, **59**(1): 67 – 69. DOI: 10.1016/0370-2693(75)90158-6.
- 4 Freedman B A, McLerran L D. Fermions and gauge vector mesons at finite temperature and density. III. The ground-state energy of a relativistic quark gas[J]. *Physical Review D*, 1977, **16**(4): 1169 – 1185. DOI: 10.1103/physrevd.16.1169.
- 5 Shuryak E V. Quark-gluon plasma and hadronic production of leptons, photons and psions[J]. *Physics Letters B*, 1978, **78**(1): 150 – 153. DOI: 10.1016/0370-2693(78)90370-2.
- 6 Kapusta J I. Quantum chromodynamics at high temperature[J]. *Nuclear Physics B*, 1979, **148**(3 – 4): 461 – 498. DOI: 10.1016/0550-3213(79)90146-9.
- 7 Aoki Y, Endrodi G, Fodor Z, *et al.* The order of the quantum chromodynamics transition predicted by the standard model of particle physics[J]. *Nature*, 2006, **443** (7112): 675 – 678. DOI: 10.1038/nature05120.
- 8 Aoki Y. The QCD transition temperature: results with physical masses in the continuum limit[J]. *Physics Letters B*, 2006, **643**(1): 46 – 54. DOI: 10.1016/j.physletb.2006.10.021.
- 9 Aoki Y, Borsanyi S, Durr S, *et al.* The QCD transition temperature: results with physical masses in the continuum limit II[J]. *Journal of High Energy Physics*, 2009, **2009**(06): 088. DOI: 10.1088/1126-6708/2009/06/088.
- 10 Bazavov A, Bhattacharya T, Cheng M, *et al.* Chiral and deconfinement aspects of the QCD transition[J]. *Physical Review D*, 2012, **85**(5): 054503. DOI: 10.1103/physrevd.85.054503.
- 11 Bazavov A, Bhattacharya T, DeTar C, *et al.* Equation of state in (2+1)-flavor QCD[J]. *Physical Review D*, 2014, **90**(9): 094503. DOI: 10.1103/PhysRevD.90.094503.
- 12 Bhattacharya T, Buchoff M I, Christ N H, *et al.* QCD phase transition with chiral quarks and physical quark

- masses[J]. Physical Review Letters, 2014, **113**(8): 082001. DOI: 10.1103/PhysRevLett.113.082001.
- 13 Borsanyi S, Fodor Z, Guenther J N, *et al.* QCD crossover at finite chemical potential from lattice simulations[J]. Physical Review Letters, 2020, **125**(5): 052001. DOI: 10.1103/physrevlett.125.052001.
 - 14 Stephanov M A. QCD phase diagram: an overview[J]. PoS, 2006, **LAT2006**: 024. DOI: 10.22323/1.032.0024.
 - 15 Stephanov M A. QCD phase diagram and the critical point [J]. International Journal of Modern Physics A, 2005, **20** (19): 4387 – 4392. DOI: 10.1142/s0217751x05027965.
 - 16 Fukushima K, Sasaki C. The phase diagram of nuclear and quark matter at high baryon density[J]. Progress in Particle and Nuclear Physics, 2013, **72**: 99 – 154. DOI: 10.1016/j.pnpnp.2013.05.003.
 - 17 Baym G, Hatsuda T, Kojo T, *et al.* From hadrons to quarks in neutron stars: a review[J]. Reports on Progress in Physics, 2018, **81**(5): 056902. DOI: 10.1088/1361-6633/aaae14.
 - 18 杜轶伦, 李程明, 史潮, 等. 基于有效场论的QCD相图研究 [J]. 核技术, 2023, **46**(4): 040009. DOI: 10.11889/j.0253-3219.2023.hjs.46.040009.
DU Yilun, LI Chengming, SHI Chao, *et al.* Review of QCD phase diagram analysis using effective field theories [J]. Nuclear Techniques, 2023, **46**(4): 040009. DOI: 10.11889/j.0253-3219.2023.hjs.46.040009.
 - 19 朱洲润, 赵彦清, 侯德富. QCD相结构的全息模型研究 [J]. 核技术, 2023, **46**(4): 040007. DOI: 10.11889/j.0253-3219.2023.hjs.46.040007.
ZHU Zhou-run, ZHAO Yanqing, HOU Defu. QCD phase structure from holographic models[J]. Nuclear Techniques, 2023, **46**(4): 040007. DOI: 10.11889/j.0253-3219.2023.hjs.46.040007.
 - 20 尹诗, 谈阳阳, 付伟杰. 临界现象与泛函重整化群[J]. 核技术, 2023, **46**(4): 040002. DOI: 10.11889/j.0253-3219.2023.hjs.46.040002.
YIN Shi, TAN Yangyang, FU Weijie. Critical phenomena and functional renormalization group[J]. Nuclear Techniques, 2023, **46**(4): 040002. DOI: 10.11889/j.0253-3219.2023.hjs.46.040002.
 - 21 丁亨通, 李胜泰, 刘俊宏. 强磁场下的格点QCD研究进展 [J]. 核技术, 2023, **46**(4): 040008. DOI: 10.11889/j.0253-3219.2023.hjs.46.040008.
DING Hengtong, LI Shengtai, LIU Junhong. Progress on QCD properties in strong magnetic fields from lattice QCD[J]. Nuclear Techniques, 2023, **46**(4): 040008. DOI: 10.11889/j.0253-3219.2023.hjs.46.040008.
 - 22 曹高清. 极强磁场与QCD相图[J]. 核技术, 2023, **46**(4): 040003. DOI: 10.11889/j.0253-3219.2023.hjs.46.040003.
CAO Gaoqing. Extremely strong magnetic field and QCD phase diagram[J]. Nuclear Techniques, 2023, **46**(4): 040003. DOI: 10.11889/j.0253-3219.2023.hjs.46.040003.
 - 23 Luo X F, Xu N. Search for the QCD critical point with fluctuations of conserved quantities in relativistic heavy-ion collisions at RHIC: an overview[J]. Nuclear Science and Techniques, 2017, **28**(8): 112. DOI: 10.1007/s41365-017-0257-0.
 - 24 Bzdak A. Mapping the phases of quantum chromodynamics with beam energy scan[J]. Physics Reports, 2020, **853**: 1 – 87. DOI: 10.1016/j.physrep.2020.01.005.
 - 25 Abelev B I, Aggarwal M M, Ahammed Z, *et al.* Properties of QCD matter at high baryon density[EB/OL]. 2022: Springer.
 - 26 Fu W J. QCD at finite temperature and density within the $\overline{\text{IRG}}$ approach: an overview[J]. Communications in Theoretical Physics, 2022, **74**(9): 097304. DOI: 10.1088/1572-9494/ac86be.
 - 27 Pandav A, Mallick D, Mohanty B. Search for the QCD critical point in high energy nuclear collisions[J]. Progress in Particle and Nuclear Physics, 2022, **125**: 103960. DOI: 10.1016/j.pnpnp.2022.103960.
 - 28 张宇, 张定伟, 罗晓峰. 相对论重离子碰撞中QCD相图的实验研究 [J]. 核技术, 2023, **46**(4): 040001. DOI: 10.11889/j.0253-3219.2023.hjs.46.040001.
ZHANG Yu, ZHANG Dingwei, LUO Xiaofeng. Experimental study of the QCD phase diagram in relativistic heavy-ion collisions[J]. Nuclear Techniques, 2023, **46**(4): 040001. DOI: 10.11889/j.0253-3219.2023.hjs.46.040001.
 - 29 尹伊. BEST合作组QCD相图研究进展 [J]. 核技术, 2023, **46**(4): 040010. DOI: 10.11889/j.0253-3219.2023.hjs.46.040010.
YIN Yi. The BEST framework for exploring the QCD phase diagram: progress summary[J]. Nuclear Techniques, 2023, **46**(4): 040010. DOI: 10.11889/j.0253-3219.2023.hjs.46.040010.
 - 30 吴元芳, 李笑冰, 陈丽珠, 等. 相对论重离子碰撞中确定QCD相边界的若干问题 [J]. 核技术, 2023, **46**(4): 040006. DOI: 10.11889/j.0253-3219.2023.hjs.46.040006.
WU Yuanfang, LI Xiaobing, CHEN Lizhu, *et al.* Several problems in determining the QCD phase boundary by

- relativistic heavy ion collisions[J]. Nuclear Techniques, 2023, **46**(4): 040006. DOI: 10.11889/j.0253-3219.2023.hjs.46.040006.
- 31 Asakawa M, Kitazawa M. Fluctuations of conserved charges in relativistic heavy ion collisions: an introduction [J]. Progress in Particle and Nuclear Physics, 2016, **90**: 299 – 342. DOI: 10.1016/j.pnpnp.2016.04.002.
- 32 许坤, 黄梅. QCD 临界终点与重子数扰动[J]. 核技术, 2023, **46**(4): 040005. DOI: 10.11889/j.0253-3219.2023.hjs.46.040005.
- XU Kun, HUANG Mei. QCD critical end point and baryon number fluctuation[J]. Nuclear Techniques, 2023, **46**(4): 040005. DOI: 10.11889/j.0253-3219.2023.hjs.46.040005.
- 33 Adam J, Adamczyk L, Adams J R, *et al.* Nonmonotonic energy dependence of net-proton number fluctuations[J]. Physical Review Letters, 2021, **126**(9): 092301. DOI: 10.1103/physrevlett.126.092301.
- 34 Stephanov M A. Sign of kurtosis near the QCD critical point[J]. Physical Review Letters, 2011, **107**(5): 052301. DOI: 10.1103/PhysRevLett.107.052301.
- 35 吴善进, 宋慧超. QCD 临界点附近的动力学临界涨落 [J]. 核技术, 2023, **46**(4): 040004. DOI: 10.11889/j.0253-3219.2023.hjs.46.040004.
- WU Shanjin, SONG Huichao. Critical dynamical fluctuations near the QCD critical point[J]. Nuclear Techniques, 2023, **46**(4): 040004. DOI: 10.11889/j.0253-3219.2023.hjs.46.040004.
- 36 Abelev B I, Aggarwal M M, Ahammed Z, *et al.* Observation of an antimatter hypernucleus[J]. Science, 2010, **328**(5974): 58 – 62. DOI: 10.1126/science.1183980.
- 37 Agakishiev H, Aggarwal M M, Ahammed Z, *et al.* Observation of the antimatter helium-4 nucleus[J]. Nature, 2011, **473**(7347): 353 – 356. DOI: 10.1038/nature10079.
- 38 Adam J, Adamová D, Aggarwal M M, *et al.* Precision measurement of the mass difference between light nuclei and anti-nuclei[J]. Nature Physics, 2015, **11**(10): 811 – 814. DOI: 10.1038/nphys3432.
- 39 Adam J, Adamczyk L, Adams J R, *et al.* Measurement of the mass difference and the binding energy of the hypertriton and antihypertriton[J]. Nature Physics, 2020, **16**(4): 409 – 412. DOI: 10.1038/s41567-020-0799-7.
- 40 Sun K J. Probing QCD critical fluctuations from light nuclei production in relativistic heavy-ion collisions[J]. Physics Letters B, 2017, **774**: 103 – 107. DOI: 10.1016/j.physletb.2017.09.056.
- 41 Sun K J, Chen L W, Ko C M, *et al.* Light nuclei production as a probe of the QCD phase diagram[J]. Physics Letters B, 2018, **781**: 499 – 504. DOI: 10.1016/j.physletb.2018.04.035.
- 42 Sun K J, Li F, Ko C M. Effects of QCD critical point on light nuclei production[J]. Physics Letters B, 2021, **816**: 136258. DOI: 10.1016/j.physletb.2021.136258.
- 43 Shuryak E, Torres-Rincon J M. Baryon clustering at the critical line and near the hypothetical critical point in heavy-ion collisions[J]. Physical Review C, 2019, **100**(2): 024903. DOI: 10.1103/physrevc.100.024903.
- 44 Shuryak E, Torres-Rincon J M. Light-nuclei production and search for the QCD critical point[J]. The European Physical Journal A, 2020, **56**(9): 241. DOI: 10.1140/epja/s10050-020-00244-3.
- 45 Berdnikov B, Rajagopal K. Slowing out of equilibrium near the QCD critical point[J]. Physical Review D, 2000, **61**(10): 105017. DOI: 10.1103/physrevd.61.105017.
- 46 Mishustin I N. Nonequilibrium phase transition in rapidly expanding matter[J]. Physical Review Letters, 1999, **82** (24): 4779 – 4782. DOI: 10.1103/physrevlett.82.4779.
- 47 Chomaz P, Colonna M, Randrup J. Nuclear spinodal fragmentation[J]. Physics Reports, 2004, **389**(5 – 6): 263 – 440. DOI: 10.1016/j.physrep.2003.09.006.
- 48 Sasaki C, Friman B, Redlich K. Density fluctuations in the presence of spinodal instabilities[J]. Physical Review Letters, 2007, **99**(23): 232301. DOI: 10.1103/PhysRevLett.99.232301.
- 49 Steinheimer J, Randrup J. Spinodal amplification of density fluctuations in fluid-dynamical simulations of relativistic nuclear collisions[J]. Physical Review Letters, 2012, **109**(21): 212301. DOI: 10.1103/PhysRevLett.109.212301.
- 50 Lacey R A. Indications for a critical end point in the phase diagram for hot and dense nuclear matter[J]. Physical Review Letters, 2015, **114**(14): 142301. DOI: 10.1103/PhysRevLett.114.142301.
- 51 Seck F, Galatyuk T, Mukherjee A, *et al.* Dilepton signature of a first-order phase transition[J]. Physical Review C, 2022, **106**: 014904. DOI: 10.1103/physrevc.106.014904.
- 52 Batyuk P, Blaschke D, Bleicher M, *et al.* Event simulation based on three-fluid hydrodynamics for collisions at energies available at the Dubna Nuclotron-based Ion Collider Facility and at the Facility for Antiproton and Ion

- Research in Darmstadt[J]. Physical Review C, 2016, **94** (4): 044917. DOI: 10.1103/physrevc.94.044917.
- 53 Steinheimer J, Randrup J, Koch V. Non-equilibrium phase transition in relativistic nuclear collisions: importance of the equation of state[J]. Physical Review C, 2014, **89**(3): 034901. DOI: 10.1103/physrevc.89.034901.
- 54 Sun K J, Ko C M, Li F, *et al.* Enhanced yield ratio of light nuclei in heavy ion collisions with a first-order chiral phase transition[J]. The European Physical Journal A, 2021, **57**(11): 313. DOI: 10.1140/epja/s10050-021-00607-4.
- 55 Murase K, Hirano T. Hydrodynamic fluctuations and dissipation in an integrated dynamical model[J]. Nuclear Physics A, 2016, **956**: 276 - 279. DOI: 10.1016/j.nuclphysa.2016.01.011.
- 56 Nahrgang M, Bluhm M, Schäfer T, *et al.* Toward the description of fluid dynamical fluctuations in heavy-ion collisions[J]. Acta Physica Polonica B Proceedings Supplement, 2017, **10**(3): 687. DOI: 10.5506/aphyspolbsupp.10.687.
- 57 Hirano T, Kurita R, Murase K. Hydrodynamic fluctuations of entropy in one-dimensionally expanding system[J]. Nuclear Physics A, 2019, **984**: 44 - 67. DOI: 10.1016/j.nuclphysa.2019.01.010.
- 58 Singh M, Shen C, McDonald S, *et al.* Hydrodynamic fluctuations in relativistic heavy-ion collisions[J]. Nuclear Physics A, 2019, **982**: 319 - 322. DOI: 10.1016/j.nuclphysa.2018.10.061.
- 59 Akamatsu Y, Mazeliauskas A, Teaney D. Kinetic regime of hydrodynamic fluctuations and long time tails for a Bjorken expansion[J]. Physical Review C, 2017, **95**: 014909. DOI: 10.1103/physrevc.95.014909.
- 60 Stephanov M, Yin Y. Hydrodynamics with parametric slowing down and fluctuations near the critical point[J]. Physical Review D, 2018, **98**(3): 036006. DOI: 10.1103/physrevd.98.036006.
- 61 An X, Başar G, Stephanov M, *et al.* Relativistic hydrodynamic fluctuations[J]. Physical Review C, 2019, **100**(2): 024910. DOI: 10.1103/physrevc.100.024910.
- 62 Rajagopal K, Ridgway G W, Weller R, *et al.* Understanding the out-of-equilibrium dynamics near a critical point in the QCD phase diagram[J]. Physical Review D, 2020, **102**(9): 094025. DOI: 10.1103/physrevd.102.094025.
- 63 Nahrgang M, Leupold S, Herold C, *et al.* Nonequilibrium chiral fluid dynamics including dissipation and noise[J]. Physical Review C, 2011, **84**(2): 024912. DOI: 10.1103/physrevc.84.024912.
- 64 Herold C, Nahrgang M, Mishustin I, *et al.* Chiral fluid dynamics with explicit propagation of the Polyakov loop [J]. Physical Review C, 2013, **87**: 014907. DOI: 10.1103/physrevc.87.014907.
- 65 Herold C, Nahrgang M, Yan Y P, *et al.* Net-baryon number variance and kurtosis within nonequilibrium chiral fluid dynamics[J]. Journal of Physics G: Nuclear and Particle Physics, 2014, **41**(11): 115106. DOI: 10.1088/0954-3899/41/11/115106.
- 66 Xu J, Song T, Ko C M, *et al.* Elliptic flow splitting as a probe of the QCD phase structure at finite baryon chemical potential[J]. Physical Review Letters, 2014, **112** (1): 012301. DOI: 10.1103/PhysRevLett.112.012301.
- 67 Li F, Ko C M. Spinodal instabilities of baryon-rich quark-gluon plasma in the Polyakov-Nambu-Jona-Lasinio model [J]. Physical Review C, 2016, **93**(3): 035205. DOI: 10.1103/physrevc.93.035205.
- 68 Nambu Y, Jona-Lasinio G. Dynamical model of elementary particles based on an analogy with superconductivity. I[J]. Physical Review, 1961, **122**(1): 345 - 358. DOI: 10.1103/physrev.122.345.
- 69 Nambu Y, Jona-Lasinio G. Dynamical model of elementary particles based on an analogy with superconductivity. II[J]. Physical Review, 1961, **124**(1): 246 - 254. DOI: 10.1103/physrev.124.246.
- 70 Olive K A, Steigman G, Walker T P. Primordial nucleosynthesis: theory and observations[J]. Physics Reports, 2000, **333 - 334**: 389 - 407. DOI: 10.1016/s0370-1573(00)00031-4.
- 71 Bennett M J, Pope J K, Beavis D, *et al.* Light nuclei production in relativistic Au+nucleus collisions[J]. Physical Review C, 1998, **58**(2): 1155 - 1164. DOI: 10.1103/physrevc.58.1155.
- 72 Armstrong T A, Barish K N, Batsouli S, *et al.* Proton and deuteron production in Au+Au reactions at 11.6 AGeV/c [J]. Physical Review C, 1999, **60**(6): 064901. DOI: 10.1103/PhysRevC.60.064901.
- 73 Armstrong T A, Barish K N, Batsouli S, *et al.* Antideuteron yield at the AGS and coalescence implications[J]. Physical Review Letters, 2000, **85**(13): 2685 - 2688. DOI: 10.1103/physrevlett.85.2685.
- 74 Armstrong T A, Barish K N, Batsouli S, *et al.* Measurements of light nuclei production in 11.5 AGeV/c Au+Pb heavy-ion collisions[J]. Physical Review C, 2000.

- 61(6): 064908. DOI: 10.1103/PhysRevC.61.064908.
- 75 Adler C, Ahammed Z, Allgower C, *et al.* Anti-deuteron and anti-He-3 production in $\sqrt{s_{NN}}=130$ -GeV Au+Au collisions[J]. Physical Review Letters, 2001, **87**(26): 262301. DOI: 10.1103/PhysRevLett.87.262301.
 - 76 Adler S S, Afanasiev S, Aidala C, *et al.* Deuteron and antideuteron production in Au+Au collisions at square root of $\sqrt{s_{NN}}=200$ GeV[J]. Physical Review Letters, 2005, **94**(12): 122302. DOI: 10.1103/PhysRevLett.94.122302.
 - 77 Arsene I, Bearden I G, Beavis D, *et al.* Rapidity dependence of deuteron production in central Au+Au collisions at $\sqrt{s_{NN}}=200$ GeV[J]. Physical Review C, 2011, **83**(4): 044906. DOI: 10.1103/PhysRevC.83.044906.
 - 78 Adam J, Adamova D, Aggarwal M M, *et al.* Production of light nuclei and anti-nuclei in pp and Pb-Pb collisions at energies available at the CERN Large Hadron Collider[J]. Physical Review C, 2016, **93**(2): 024917. DOI: 10.1103/PhysRevC.93.024917.
 - 79 Adamczyk L, Adkins J K, Agakishiev G, *et al.* Measurement of elliptic flow of light nuclei at $\sqrt{s_{NN}}=200$, 62.4, 39, 27, 19.6, 11.5, and 7.7 GeV at the BNL Relativistic Heavy Ion Collider[J]. Physical Review C, 2016, **94**(3): 034908. DOI: 10.1103/PhysRevC.94.034908.
 - 80 Acharya S, Adamová D, Adolfsen J, *et al.* Measurement of deuteron spectra and elliptic flow in Pb-Pb collisions at $\sqrt{s_{NN}}=2.76$ TeV at the LHC[J]. The European Physical Journal C, 2017, **77**(10): 658. DOI: 10.1140/epjc/s10052-017-5222-x.
 - 81 Acharya S, Adam J, Adamová D, *et al.* Production of deuterons, tritons, ^3He nuclei, and their antinuclei in pp collisions at $s=0.9$, 2.76, and 7 TeV[J]. Physical Review C, 2018, **97**(2): 024615. DOI: 10.1103/PhysRevC.97.024615.
 - 82 Acharya S, Adamova D, Adhya S P, *et al.* Multiplicity dependence of (anti-)deuteron production in pp collisions at $\sqrt{s}=7$ TeV[J]. Physics Letters B, 2019, **794**: 50 - 63. DOI: 10.1016/j.physletb.2019.05.028.
 - 83 Adam J, Adamczyk L, Adams J R, *et al.* Beam energy dependence of (anti-)deuteron production in Au+Au collisions at the BNL Relativistic Heavy Ion Collider[J]. Physical Review C, 2019, **99**(6): 064905. DOI: 10.1103/PhysRevC.99.064905.
 - 84 Acharya S, Adamova D, Adhya S P, *et al.* Multiplicity dependence of light (anti-)nuclei production in p-Pb collisions at $\sqrt{s_{NN}}=5.02$ TeV[J]. Physics Letters B, 2020, **800**: 135043. DOI: 10.1016/j.physletb.2019.135043.
 - 85 Acharya S, Adamova D, Adhya S P, *et al.* Measurement of the (anti-) ^3He elliptic flow in Pb-Pb collisions at $\sqrt{s_{NN}}=5.02$ TeV[J]. Physics Letters B, 2020, **805**: 135414. DOI: 10.1016/j.physletb.2020.135414.
 - 86 Acharya S, Adamova D, Adhya S P, *et al.* Production of (anti-) ^3He and (anti-) ^3H in p-Pb collisions at $\sqrt{s_{NN}}=5.02$ TeV[J]. Physical Review C, 2020, **101**(4): 044906. DOI: 10.1103/PhysRevC.101.044906.
 - 87 Acharya S, Adamová D, Adler A, *et al.* (Anti-) deuteron production in pp collisions at $\sqrt{s}=13$ TeV[J]. The European Physical Journal C, 2020, **80**(9): 889. DOI: 10.1140/epjc/s10052-020-8256-4.
 - 88 Acharya S, Adamova D, Adhya S P, *et al.* Elliptic and triangular flow of (anti)deuterons in Pb-Pb collisions at $\sqrt{s_{NN}}=5.02$ TeV[J]. Physical Review C, 2020, **102**(5): 055203. DOI: 10.1103/PhysRevC.102.055203.
 - 89 Cho S, Furumoto T, Hyodo T, *et al.* Identifying multiquark hadrons from heavy ion collisions[J]. Physical Review Letters, 2011, **106**(21): 212001. DOI: 10.1103/physrevlett.106.212001.
 - 90 Sungtae Cho. Exotic hadrons from heavy ion collisions [J]. Progress in Particle and Nuclear Physics, 2017, **95**: 279 - 322. DOI: 10.1016/j.ppnp.2017.02.002.
 - 91 Everett D, Oliinychenko D, Luzum M, *et al.* Role of bulk viscosity in deuteron production in ultrarelativistic nuclear collisions[J]. Physical Review C, 2022, **106**(6): 064901. DOI: 10.1103/PhysRevC.106.064901.
 - 92 Blum K, Ng K C Y, Sato R, *et al.* Cosmic rays, antihelium, and an old navy spotlight[J]. Physical Review D, 2017, **96**(10): 103021. DOI: 10.1103/physrevd.96.103021.
 - 93 Poulin V, Salati P, Cholis I, *et al.* Where do the AMS-02 antihelium events come from? [J]. Physical Review D, 2019, **99**(2): 023016. DOI: 10.1103/physrevd.99.023016.
 - 94 Tomlinson J, Gebhardt H S G, Jeong D. Fast calculation of the nonlinear redshift-space galaxy power spectrum including selection bias[J]. Physical Review D, 2020, **101**(10): 103528. DOI: 10.1103/physrevd.101.103528.
 - 95 Acharya S, Adamová D, Adler A, *et al.* Measurement of the low-energy antideuteron inelastic cross section[J]. Physical Review Letters, 2020, **125**(16): 162001. DOI: 10.1103/physrevlett.125.162001.
 - 96 von Doetinchem P, Perez K, Aramaki T, *et al.* Cosmic-ray

- antinuclei as messengers of new physics: status and outlook for the new decade[J]. *Journal of Cosmology and Astroparticle Physics*, 2020, **2020**: 035. DOI: 10.1088/1475-7516/2020/08/035.
- 97 Saffold N. Cosmic antihelium-3 nuclei sensitivity of the GAPS experiment[J]. *Astroparticle Physics*, 2021, **130**: 102580. DOI: 10.1016/j.astropartphys.2021.102580.
- 98 Csernai L, Kapusta J I. Entropy and cluster production in nuclear collisions[J]. *Physics Reports*, 1986, **131**(4): 223 – 318. DOI: 10.1016/0370-1573(86)90031-1.
- 99 Chen J H, Keane D, Ma Y G, *et al.* Antinuclei in heavy-ion collisions[J]. *Physics Reports*, 2018, **760**: 1 – 39. DOI: 10.1016/j.physrep.2018.07.002.
- 100 Ono A. Dynamics of clusters and fragments in heavy-ion collisions[J]. *Progress in Particle and Nuclear Physics*, 2019, **105**: 139 – 179. DOI: 10.1016/j.pnpnp.2018.11.001.
- 101 Braun-Munzinger P, Dönigus B. Loosely-bound objects produced in nuclear collisions at the LHC[J]. *Nuclear Physics A*, 2019, **987**: 144 – 201. DOI: 10.1016/j.nuclphysa.2019.02.006.
- 102 Andronic A. Production of light nuclei, hypernuclei and their antiparticles in relativistic nuclear collisions[J]. *Physics Letters B*, 2011, **697**(3): 203 – 207. DOI: 10.1016/j.physletb.2011.01.053.
- 103 Andronic A, Braun-Munzinger P, Redlich K, *et al.* Decoding the phase structure of QCD via particle production at high energy[J]. *Nature*, 2018, **561**(7723): 321 – 330. DOI: 10.1038/s41586-018-0491-6.
- 104 Butler S T, Pearson C A. Deuterons from high-energy proton bombardment of matter[J]. *Physical Review*, 1963, **129**(2): 836 – 842. DOI: 10.1103/physrev.129.836.
- 105 Kapusta J I. Mechanisms for deuteron production in relativistic nuclear collisions[J]. *Physical Review C*, 1980, **21**(4): 1301 – 1310. DOI: 10.1103/physrevc.21.1301.
- 106 Scheibl R, Heinz U. Coalescence and flow in ultrarelativistic heavy ion collisions[J]. *Physical Review C*, 1999, **59**(3): 1585 – 1602. DOI: 10.1103/physrevc.59.1585.
- 107 Chen L W, Ko C M, Li B A. Light clusters production as a probe to nuclear symmetry energy[J]. *Physical Review C*, 2003, **68**: 017601. DOI: 10.1103/physrevc.68.017601.
- 108 Chen L W, Ko C M, Li B A. Light cluster production in intermediate energy heavy-ion collisions induced by neutron-rich nuclei[J]. *Nuclear Physics A*, 2003, **729**(2 – 4): 809 – 834. DOI: 10.1016/j.nuclphysa.2003.09.010.
- 109 Steinheimer J. Hypernuclei, dibaryon and antinuclei production in high energy heavy ion collisions: thermal production vs. coalescence[J]. *Physics Letters B*, 2012, **714**(1): 85 – 91. DOI: 10.1016/j.physletb.2012.06.069.
- 110 Sun K J, Ko C M, Dönigus B. Suppression of light nuclei production in collisions of small systems at the Large Hadron Collider[J]. *Physics Letters B*, 2019, **792**: 132 – 137. DOI: 10.1016/j.physletb.2019.03.033.
- 111 Blum K, Takimoto M. Nuclear coalescence from correlation functions[J]. *Physical Review C*, 2019, **99**(4): 044913. DOI: 10.1103/physrevc.99.044913.
- 112 Bellini F, Kalweit A P. Testing production scenarios for (anti-)(hyper-) nuclei and exotica at energies available at the CERN Large Hadron Collider[J]. *Physical Review C*, 2019, **99**(5): 054905. DOI: 10.1103/physrevc.99.054905.
- 113 Danielewicz P. Quantum theory of nonequilibrium processes, I[J]. *Annals of Physics*, 1984, **152**(2): 239 – 304. DOI: 10.1016/0003-4916(84)90092-7.
- 114 Buss O, Gaitanos T, Gallmeister K, *et al.* Transport-theoretical description of nuclear reactions[J]. *Physics Reports*, 2012, **512**(1 – 2): 1 – 124. DOI: 10.1016/j.physrep.2011.12.001.
- 115 Danielewicz P, Bertsch G F. Production of deuterons and pions in a transport model of energetic heavy-ion reactions [J]. *Nuclear Physics A*, 1991, **533**(4): 712 – 748. DOI: 10.1016/0375-9474(91)90541-d.
- 116 Danielewicz P, Schuck P. Formulation of particle correlation and cluster production in heavy-ion-induced reactions[J]. *Physics Letters B*, 1992, **274**(3 – 4): 268 – 274. DOI: 10.1016/0370-2693(92)91985-I.
- 117 Acharya S, Adamova D, Adhya S P, *et al.* Hypertriton production in p-Pb collisions at $\sqrt{s_{NN}}=5.02$ TeV[J]. *Physical Review Letters*, 2022, **128**(25): 252003. DOI: 10.1103/PhysRevLett.128.252003.
- 118 Acharya S, Adamova D, Adhya S P, *et al.* First measurement of antideuteron number fluctuations at energies available at the Large Hadron Collider[EB/OL]. 2022: arXiv: 2204.10166. <https://arxiv.org/abs/2204.10166>.
- 119 Acharya S, Adamova D, Adhya S P, *et al.* Enhanced deuteron coalescence probability in jets[EB/OL]. 2022: arXiv:2211.15204. <https://arxiv.org/abs/2211.15204>.
- 120 Röpke G. Light nuclei quasiparticle energy shifts in hot and dense nuclear matter[J]. *Physical Review C*, 2009, **79**: 014002. DOI: 10.1103/physrevc.79.014002.
- 121 Sun K J, Chen L W. Production of antimatter $^5,6\text{Li}$ nuclei

- in central Au+Au collisions at $\sqrt{s_{NN}}=200$ GeV[J]. Physics Letters B, 2015, **751**: 272 - 277. DOI: 10.1016/j.physletb.2015.10.056.
- 122 Sun K J, Chen L W. Analytical coalescence formula for particle production in relativistic heavy-ion collisions[J]. Physical Review C, 2017, **95**(4): 044905. DOI: 10.1103/physrevc.95.044905.
- 123 Wu S J, Murase K, Tang S A, *et al.* Examination of background effects on the light-nuclei yield ratio in relativistic heavy-ion collisions[J]. Physical Review C, 2022, **106**(3): 034905. DOI: 10.1103/physrevc.106.034905.
- 124 Buballa M. NJL-model analysis of dense quark matter[J]. Physics Reports, 2005, **407**(4 - 6): 205 - 376. DOI: 10.1016/j.physrep.2004.11.004.
- 125 't Hooft G. Computation of the quantum effects due to a four-dimensional pseudoparticle[J]. Physical Review D, 1976, **14**(12): 3432 - 3450. DOI: 10.1103/physrevd.14.3432.
- 126 Masuda K, Hatsuda T, Takatsuka T. Hadron-quark crossover and massive hybrid stars[J]. Progress of Theoretical and Experimental Physics, 2013, **2013**(7): 073D01. DOI: 10.1093/ptep/ptt045.
- 127 Vogl U, Weise W. The Nambu and jona-lasinio model: its implications for hadrons and nuclei[J]. Progress in Particle and Nuclear Physics, 1991, **27**: 195 - 272. DOI: 10.1016/0146-6410(91)90005-9.
- 128 Lutz M, Klimt S, Weise W. Meson properties at finite temperature and baryon density[J]. Nuclear Physics A, 1992, **542**(4): 521 - 558. DOI: 10.1016/0375-9474(92)90256-j.
- 129 Bratovic N, Hatsuda T, Weise W. Role of vector interaction and axial anomaly in the PNJL modeling of the QCD phase diagram[J]. Physics Letters B, 2013, **719**(1 - 3): 131 - 135. DOI: 10.1016/j.physletb.2013.01.003.
- 130 Liu L M, Zhou W H, Xu J, *et al.* Isospin effect on quark matter instabilities[J]. Physics Letters B, 2021, **822**: 136694. DOI: 10.1016/j.physletb.2021.136694.
- 131 Ko C M, Li Q, Wang R. Relativistic Vlasov equation for heavy-ion collisions[J]. Physical Review Letters, 1987, **59**(10): 1084 - 1087. DOI: 10.1103/PhysRevLett.59.1084.
- 132 Ko C M, Li Q. Relativistic Vlasov-Uehling-Uhlenbeck model for heavy-ion collisions[J]. Physical Review C, Nuclear Physics, 1988, **37**(5): 2270 - 2273. DOI: 10.1103/physrevc.37.2270.
- 133 Wong C Y. Dynamics of nuclear fluid. VIII. Time-dependent Hartree-Fock approximation from a classical point of view[J]. Physical Review C, 1982, **25**(3): 1460 - 1475. DOI: 10.1103/physrevc.25.1460.
- 134 Sun K J, Ko C M, Cao S S, *et al.* QCD critical point from the Nambu-Jona-Lasino model with a scalar-vector interaction[J]. Physical Review D, 2021, **103**: 014006. DOI: 10.1103/physrevd.103.014006.
- 135 Sun K, Zhou W, Chen L, *et al.* Spinodal enhancement of light nuclei yield ratio in relativistic heavy ion collisions [EB/OL]. 2022: arXiv: 2205.11010. <https://arxiv.org/abs/2205.11010>.
- 136 Sun K J, Ko C M, Lin Z W. Light nuclei production in a multiphase transport model for relativistic heavy ion collisions[J]. Physical Review C, 2021, **103**(6): 064909. DOI: 10.1103/physrevc.103.064909.
- 137 Bleicher M, Zabrodin E, Spieles C, *et al.* Relativistic hadron-hadron collisions in the ultra-relativistic quantum molecular dynamics model[J]. Journal of Physics G: Nuclear and Particle Physics, 1999, **25**(9): 1859 - 1896. DOI: 10.1088/0954-3899/25/9/308.
- 138 Zhao W B, Sun K J, Ko C M, *et al.* Multiplicity scaling of light nuclei production in relativistic heavy-ion collisions [J]. Physics Letters B, 2021, **820**: 136571. DOI: 10.1016/j.physletb.2021.136571.
- 139 Adam J, Adamczyk L, Adams J R, *et al.* Beam energy dependence of triton production and yield ratio ($N_T N_p / N_d^2$) in Au+Au collisions at RHIC[EB/OL]. 2022: arXiv: 2209.08058. <https://arxiv.org/abs/2209.08058>.
- 140 Liu H, Zhang D W, He S, *et al.* Light nuclei production in Au+Au collisions at $\sqrt{s_{NN}}=5-200$ GeV from JAM model [J]. Physics Letters B, 2020, **805**: 135452. DOI: 10.1016/j.physletb.2020.135452.
- 141 Zhou W H, Liu H, Li F, *et al.* Elliptic flow splittings in the Polyakov-Nambu-Jona-Lasinio transport model[J]. Physical Review C, 2021, **104**(4): 044901. DOI: 10.1103/physrevc.104.044901.
- 142 Ma Y G. New type of double-slit interference experiment at Fermi scale[J]. Nuclear Science and Techniques, 2023, **34**(1): 16. DOI: 10.1007/s41365-023-01167-6.
- 143 Wang X N. Vector meson spin alignment by the strong force field[J]. Nuclear Science and Techniques, 2023, **34**(1): 15. DOI: 10.1007/s41365-023-01166-7.